JOURNAL OF Materials CHEMISTRY

Hexagonally organised mesoporous aluminium–oxo–hydroxide thin films prepared by the template approach. *In situ* study of the structural formation

Ludivine Pidol,[a] David Grosso,[a] Galo J. A. A. Soler-Illia,[a] Eduardo L. Crepaldi,[a] Clément Sanchez,*[a] Pierre A. Albouy,[b] Heinz Amenitsch[c] and Patrick Euzen[d]

[a]*Chimie de la Matière Condensée, UPMC–CNRS, UMR 7574, 4 place Jussieu, 75005 Paris, France. E-mail: clems@ccr.jussieu.fr*
[b]*Lab. de Physique des Solides, Université Paris-Sud, 91405 Orsay, France*
[c]*Institute of Biophysics and X-ray Structure Research, Austrian Academy of Sciences, Steyrergasse 17/VI, 8010 Graz, Austria*
[d]*Institut Francais du Pétrole, Division Cinétique et Catalyse (service RH10), 1–4 Avenue de Bois-Préau, 92500 Rueil Malmaison, France*

Received 9th October 2001, Accepted 12th December 2001
First published as an Advance Article on the web 8th February 2002

Mesoporous organised aluminium oxide based thin films have been prepared by combining the dip-coating method, the sol–gel chemistry and the template approach. The oxide network is composed of aligned-with-the-surface cylindrical pores compacted in the 2D-hexagonal *p6m* space group. $AlCl_3$ has been chosen as precursor and Brij 58 was used as structuring agent. Once deposited, films were treated to eliminate the organic surfactant and to stiffen the inorganic oxide structure. The final films are around 100 nm thick, exhibit an overall excellent optical quality, and undergo a contraction that transforms the hexagonal *p6m* original mesostructure into a centred rectangular *c2m* one, without significantly altering the degree of pore organisation. The structure was deduced from TEM and XRD in θ–2θ and transmission modes. The time-resolved formation of the film and the structure was simultaneously followed by *in situ* SAXS (synchrotron radiation) and interferometry. XRD, FTIR, ^{27}Al NMR and RBS analyses allowed characterisation of the chemical composition of the present system at different stages of its evolution. This work shows that the meso-organisation is highly humidity dependent and that as-prepared hybrid films present a significant flexibility.

1. Introduction

In terms of catalytic applications, and more specifically for acid catalysis, MCM 41 type aluminosilicate based materials present a high selectivity and a better conversion rate than amorphous aluminosilicate materials.[1] However, such mesoporous materials have the disadvantage of being expensive to synthesise in addition to being of relatively low stability. The template method used to prepare mesoporous materials with ionic surfactants was first discovered by the Mobil corporation,[2] and was enlarged by using cheaper non ionic block copolymer surfactants that lead to thicker and more stable network walls.[3–10] The use of sol–gel chemistry is versatile and allows the preparation of such materials as bulks, powders, monoliths and films. Mesoporous thin films composed of silica,[9,11–13] titania[14] and zirconia[15] organised networks have been produced using the sol–gel chemistry in the presence of block copolymer surfactants. Following a similar approach, we introduce in the present work an easy method to produce pure aluminium oxide based mesoporous thin films, that show an excellent degree of organisation before and after thermal treatment. In addition to the vast domains of application associated (optics, separation, sensors), thin films bring the advantage of being a useful system for the study of self-assembly phenomena taking place during deposition.[7,16,17] In dip-coating, the micellisation/organisation/condensation is governed by the rapid evaporation of the volatile species, simultaneously increasing the concentration in non-volatile components.[16,18] These complex processes have already been explored for silica based films where it has been underlined that the type of inorganic precursor and structuring agent, the solution ageing time (influencing the condensation degree of inorganic oligomers formed), the solution pH, the composition of the medium and the presence of air/film and film/substrate interfaces are critical parameters for the formation of the organised hybrid mesostructures.[16,19,20] Such studies are of paramount importance for the understanding of the self-assembly process and can be transposed to the preparation of bulk materials. The limiting factor of studying films lies in the fact that because of the morphology, the very low quantity of material and the rapid evaporation, it is rather difficult to obtain chemical information during deposition.

Mesoporous aluminium oxide based thin films and powders, exhibiting a poor degree of organisation, can be prepared from aluminium *sec*-butoxide and using triethanolamine[21] as complexing agent, or using the decomposition of urea.[5,10,22] In the present approach, highly organised hexagonal (*p6m*) and centred rectangular (*c2m*) films were obtained using $AlCl_3$ and Brij 58 ($C_{16}H_{33}POE_{20}$) dissolved in ethanol–water. The films were prepared by dip-coating at a constant withdrawal rate, and were subsequently treated at 220 °C, combined with an ozone atmosphere. Initial solutions were characterised by ^{27}Al NMR; as-prepared and treated films were characterised by FTIR and RBS for the chemical composition and XRD and TEM for the crystalline and mesostructures. The film formation during dip-coating was simultaneously studied by *in situ* time-resolved SAXS, informing on the structural evolution, and interferometry, giving the advancement of the evaporation. In such study, we show that formation of a well-organised structure requires the deposition in a low relative

humidity atmosphere (RH < 30%), and that the hybrid network is constructed *via* the self-assembly of poorly condensed soluble species (*i.e.* molecular or small oligomers) with block copolymer molecules at a later stage of evaporation. The obtained architecture (2D-hexagonal) remains flexible after several tens of minutes as a swelling of the lattice parameter is observed when the humidity is increased. This observation corroborates the fact that the inorganic framework is poorly condensed soon after deposition. Therefore, such as-prepared hybrid systems are not stable and thus fragile after drying. A careful treatment must be applied to enhance the condensation degree of the inorganic phase and to eliminate the organic phase, in order to prevent the complete collapsing of the meso-organisation or its transformation into a worm-like structure.

2. Experimental

2.1. Preparation of coatings

Brij 58 ($C_{16}H_{33}(OCH_2CH_2)_{20}OH$–Aldrich) was dissolved in a mixture of water and ethanol at the following molar ratio Brij 58: 0.03–0.1; EtOH: 150; H_2O: 40. This solution was ultrasonicated 15 min before anhydrous $AlCl_3$ (Prolabo) (molar ratio: 1) was slowly added to the solution at 0 °C under vigorous stirring. Once the solution had cooled down, the pH was slightly increased with NH_4OH (molar ratio 0.05 to 7—final concentration 5×10^{-3} to 0.7 mol l^{-1}). For the standard composition, corresponding to Brij 58: 0.08; EtOH: 150; H_2O: 40; $AlCl_3$: 1; NH_4OH: 0.1, the final solution pH was measured to be 1.75. Solutions were aged for 1 h under stirring and films were deposited by dip-coating on glass plates or silicon wafers under a relative humidity of 30% and at constant withdrawal speeds, ranging from 0.1 to 0.7 cm. s^{-1}. Higher rates led to thicker films and a thickness of 95 nm was measured by ellipsometry for films deposited at 0.3 cm. s^{-1}. Films were allowed to dry at ambient temperature for 1 h before being successively heated in air at 100 °C for 30 min, treated in O_3 for 45 min, heated from 100 °C to 220 °C in air with a ramp of 1 °C min^{-1}, and finally allowed to stay at 220 °C for 30 min. The O_3 treatment was intended to eliminate the organic phase and to further consolidate the oxide network by creating oxo bridges as previously reported.[23,24]

2.2. Structural characterisation

The structure of as-prepared and treated films were deduced from X-Ray Diffraction (XRD) diagrams collected in the θ–2θ mode using a conventional goniometer PW 1820 Philips (Cu-Kα radiation—acquisition time 2.5 s per 0.01° step). In such a geometry, only planes that are parallel to the substrate surface are observed. Micrographs of the treated films were obtained with a Transmission Electron Microscope (TEM) JEOL CX II apparatus. Pieces of films were scratched off the substrate, redispersed in ethanol and deposited on a carbon-coated copper grid. With this method, most of the domains lay parallel to the surface of the grid (channels coplanar to the surface). However, other orientations may be observed (*i.e.* channels normal to the surface). In the present case both orientations were found. *In situ* structural evolution of films during dip-coating have been performed in transmission mode using the synchrotron radiation (λ = 1.541 Å) of the Austrian SAXS beam-line of ELETTRA (Italy). For this experiment, a modified version of a dip-coater has been build up in order to fit the SAXS line. The substrate was kept fixed in height at an angle of 4° with respect to the incident X-ray beam; the solution was first moved up, as for the substrate to be immersed in the sol, and was then lowered to perform the coating. The structural evolution of the film during evaporation and drying was then followed by collecting the diffracted rays on a CCD camera every 2 s from the time when the top level of the solution passes the position of the X-ray incident beam. In this geometry the same area of the sample was analysed in time. Simultaneously, the advancement of the evaporation and thus the thickness evolution was followed by collecting on a second CCD camera constructive and destructive interference fringes created by the reflection of a monochromatic light on the film/substrate system. Details on such an experiment involving both techniques have been published elsewhere.[4,16,18] The whole dip-coating system was sealed in a closed cabinet equipped with a humidity sensor. The relative humidity (RH) in the dip-coater has been adjusted by allowing dry nitrogen or hot water vapour to flow within.

2.3. Chemical characterisation

The chemical environment of Al atoms within the initial solution has been studied by ^{27}Al liquid NMR (BRUKER AVANCE 400 MHz). FTIR investigations were performed on KBr pellets containing scratched pieces of films using a Nicolet 550 FT spectrophotometer. The amount of chloride present in the as-prepared and dried films has been determined using Rutherford Back Scattering (RBS) technique (van de Graaff apparatus–1.8 MeV energy). Only the amount of Cl per surface unit could be determined as the ^{27}Al signal was overlapped by the signal of the ^{28}Si from the substrate.

3. Results

3.1. θ–2θ and 2D-XRD investigations

Fig. 1(a) shows the θ–2θ XRD diagram of the as-prepared films deposited from the standard solution, in which a single diffracted peak is observed at d = 67 Å. The peak, characteristic of an organisation at the mesoscopic scale, can be observed from 0.03 to 0.1 molar ratio in Brij 58. This peak corresponds to the (01) diffraction of a typical 2D-hexagonal *p6m* mesostructure as shown in Fig. 1 (inset). The stability of

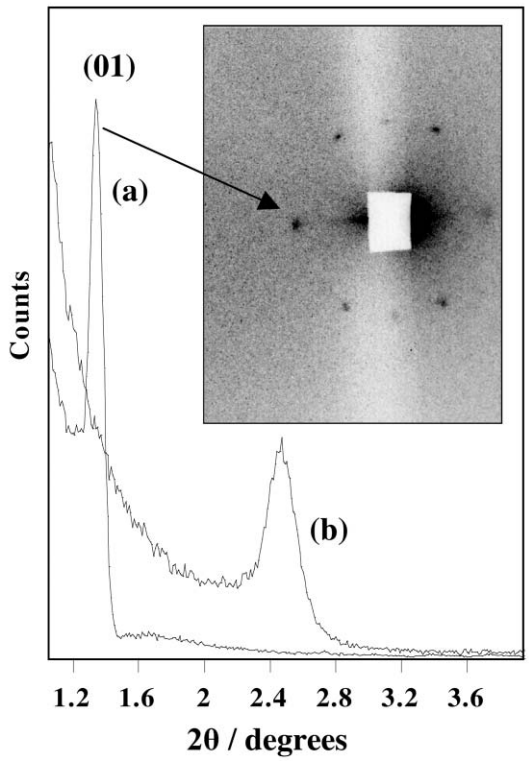

Fig. 1 Low-angle XRD patterns recorded in θ–2θ scan mode using Cu-Kα radiation for the as-prepared (a) and treated film (b) deposited on silicon wafers. Inset: 2D-XRD pattern of an as-prepared film showing the typical diffraction spots of 2D-hexagonal *p6m* structure.

the meso-organisation with time varies with the amount of NH_4OH added in the initial solution. In absence of ammonium hydroxide, the organisation is stable up to 1 day. When the molar ratio of NH_4OH is fixed at and above 0.1, the organisation is retained up to several days. Just above 0.1, one observes a partial flocculation induced by a local high concentration of base that promotes hydrolysis–condensation. After several tens of minutes of stirring, the solution becomes homogeneous and clear again, suggesting that re-dissolution takes place. Films prepared with these latter preparations lead to similar organisation to those with 0.1 molar equivalents of base. In the present paper, only films prepared with the standard solution, typically Brij 58: 0.08; EtOH: 150; H_2O: 40; $AlCl_3$: 1; NH_4OH: 0.1 molar ratio, are presented. The XRD diagram corresponding to the film treated as described in the Experimental section is displayed in Fig. 1(b). The single peak observed at $d = 36$ Å confirms that the meso-organisation of the as-prepared film is retained after 220 °C. The decrease of the *d*-spacing is due to the shrinkage induced by the treatment, a common phenomenon systematically observed on meso-structure bulks and films upon elimination of the structuring agent and rigidification of the inorganic network. Concerning SiO_2, TiO_2 and ZrO_2 films, this contraction is unidirectional and applies normal to the surface only.[14,15,25,26] The oxide based films adopt a 2D-hexagonal (*p6m*) arrangement of rod-like micelles, which classically turns into centred rectangular (*c2m*) structure upon this uni-directional shrinkage. Knowing this, the peak observed with the as-prepared film can be indexed (10) in the *p6m* space group, which becomes (02) in the *c2m* space group after treatment. In the present case the contraction corresponds to 46% in the direction normal to the surface. Above 250 °C, the mesostructure can no longer be detected by XRD and suggest that the pore network has collapsed.

XRD diagrams recorded at wide angles on treated films, clearly exhibited no diffraction (that would be characteristic of typical Boehmite AlOOH or Gibbsite $Al(OH)_3$ crystalline phases), suggesting that the inorganic network is likely composed of an amorphous aluminium oxo–hydroxide-based phase.

3.2. TEM investigation

The micrographs corresponding to pieces of a film treated as described previously are displayed in Fig. 2(a) and 2(b) with the modulus of the Fourier transform corresponding to the local diffraction pattern. One clearly observes the contracted hexagonal arrangement of pores of the [001] zone axis in Fig. 2(a), and the alignment of cylindrical pores of the [110] zone axis in Fig. 2(b). These results confirm that the treated film is composed of centred rectangular organised (*c2m*) domains resulting from the contraction of initial hexagonal (*p6m*) domains, which applies preferentially normal to the substrate. In Fig. 2(a), characteristic distances between pores were measured to be 66 Å in the [100] direction, 74 Å in the [010] direction and 51 Å in the [110] direction, while in Fig. 2(b), the characteristic distance between channels was measured to be 46 Å. The pattern in Fig. 2(b) corresponds thus to an area that was cut in the [110] direction, which corresponds to less dense planes. The 74 Å distance in the [010] direction, deduced by direct measurement on the TEM images, corresponds exactly to double the 37 Å obtained by XRD in θ–2θ mode (Fig. 1(b)), despite the focusing effects often observed with TEM analysis. As a result, one can say that the contraction induced by the treatment was 45% in the direction normal to the surface and 15% in the directions that are coplanar to the surface. For comparison, it is important to notice that SiO_2, ZrO_2 and TiO_2 films with similar 2D-hexagonal structures undergo a smaller lateral contraction than the latter aluminium oxide based system.[7,14,15]

3.3. ^{27}Al Liquid NMR investigation

In the initial solution, the pH is close to 1.75, and a high amount of water ($H_2O/Al = 40$) is present. The ^{27}Al liquid NMR spectrum of a 2 days old standard solution clearly exhibits the characteristic signal of hexacoordinated aluminium species (a single intense and well-defined peak at 0.76 ppm, in addition to the probe signal at 57 ppm),[27] suggesting that the initial solution contains only six-fold coordination Al entities. In principle no distinction can be made between $Al(OH_2)_6^{3+}$ and $Al(OH)(OH_2)_5^{2+}$ species, that should appear as a minor perturbation in the baseline. According to the speciation diagram of aqueous Al^{3+} at 25 °C, $Al(OH_2)_6^{3+}$ species are represented in the majority in the initial solution. However, it should be noted that Al^{3+} cations are the most acidic species in the system. Thus, the pH reduction is due to hydrolysis of $Al(OH_2)_6^{3+}$ to $Al(OH)(OH_2)_5^{2+}$, and related partially condensed species such as $Al_2(OH)_2^{4+}$.[28] In such conditions, one expects to have mainly (around 90%, in view of the pH) the hexaaquo molecular entities in solution. The low degree of condensation accounts for the stability of the solutions (organised films can be obtained even with several weeks aged solutions). In order to have an idea of the pH variation taking place in the wet film during dip-coating, the initial solution was allowed to evaporate inside a rotating evaporator and the pH was measured using a pH meter at different stages of liquid phase loss. The initial pH of 1.75 decreases and reaches the value of 0 when 90% weight of solvent is lost. This is due to the preferential fast evaporation of ethanol and the related increase of HCl concentration (the HCl–water system forms an azeotropic mixture at 5% HCl). Therefore one can affirm that the departure of HCl is not complete and takes

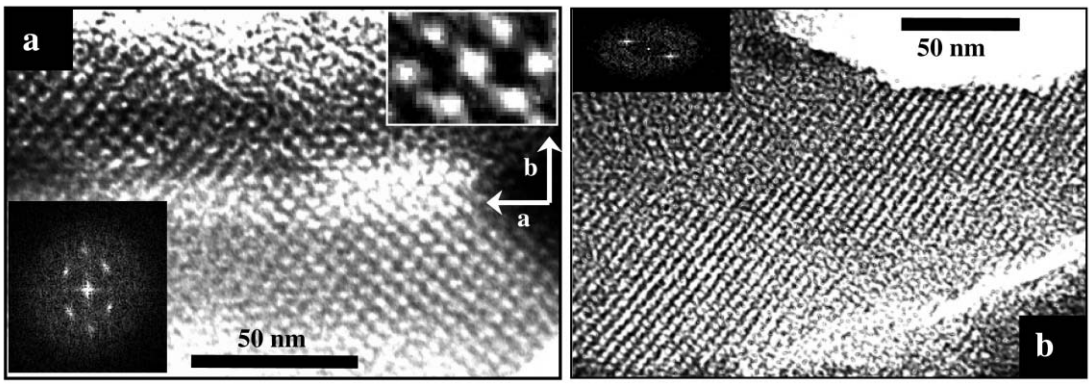

Fig. 2 TEM images of film pieces that have been scratched from the substrate. View along the [001] (a) and [110] (b) zone axes of the rectangular cell; the detailed area is magnified. Inset in parts (a) and (b) are moduli of Fourier transform of the TEM images.

place during ageing at the later stage of the film formation process (after the drying line).

3.4. RBS and FTIR investigations

The partial hydrolysis of aluminium cations in solution is responsible for the release of HCl molecules. RBS analysis performed on as-prepared 2 day old films shows only traces of chloride, meaning that most of the Cl^- ions have departed from the film during the ageing stage. This revealed that Cl^- ions are not complexing aluminium in the dry material. This result is substantially different from the titania system recently reported.[14] Further and progressive hydrolysis–condensation of the inorganic phase is induced by this HCl evaporation.

The FTIR spectra of as-prepared films revealed large quantities of water and OH groups (strong absorption at 3435 cm^{-1} for ν OH with an additional shoulder at 3250 cm^{-1} and a peak 1610 cm^{-1} characteristic of H_2O).[29,30] The typical absorption of the PEO and alkyl groups (ν C–O at 1110 cm^{-1},[31] and ν C–H at 3010 and 2925 cm^{-1}) of the Brij 58 surfactant, are also well defined. The absorption corresponding to ν Al–O at 670 cm^{-1} is present, suggesting that Al oxo–hydroxide intermediates have been hydrolysed and partly condensed during drying. The band characteristic of Al–OH at about 1100 cm^{-1} is overlapped with the ν C–O at 1110 cm^{-1}. After treatment bands corresponding to the surfactant can no longer be observed, and the intensity of ν Al–O increases while those of OH and H_2O decrease, confirming the degradation of organics and the further condensation of the inorganic framework. Furthermore, no signal corresponding to residual carbonate/carboxylate species were observed by FTIR after full treatment. The first thermal treatment at 100 °C favours the departure of residual HCl and water molecules in order to promote further condensation and stiffening of the inorganic phase, while the surfactant remains within the pores, acting as scaffolding[32] to withstand the collapsing of the structure. The O_3 treatment allows a soft degradation of the surfactant molecules by oxidation without affecting the mesostructure. This latter ozone treatment has been reported to be highly efficient for the degradation of organics.[23,24] At this stage a sharp intense band at 1386 cm^{-1} assigned to nitrate is present as a result of the oxidation of ammonia and N_2 from the atmosphere by O_3. Nitrate can easily be eliminated from the system by water washing. Finally, the film is treated at 220 °C for further consolidation.[23,24]

3.5. Time-resolved SAXS and interferometry *in situ* investigation

The structural evolution of the film has been followed by *in situ* time-resolved SAXS and the corresponding diffraction patterns are displayed in Fig. 3 (RH = 25%). Simultaneously, the film thickness decreasing with time, associated with the liquid phase evaporation, has been followed from the constructive and destructive interferometry fringes. As shown in Fig. 3, the last interference fringe (drying line) is observed 30 s after deposition; thus most of the solvent has left the system after this period of 30 s. This rapid evaporation process can be divided in two steps: the first one (faster) corresponding to narrower fringe separation can be attributed to the evaporation of the more volatile EtOH, while the second (slower) can be attributed to the departure of water.[16] As the initial system contains a high quantity of HCl, one expects the thin layer to reach a maximal acidity during deposition (evaporation of first EtOH induces a HCl concentration in the early stage, followed by the evaporation of HCl and H_2O in a later stage). However, it is difficult to predict exactly when the pH attains its minimal point because of the presence of both azeotropic H_2O–EtOH and HCl–H_2O mixtures,[33] as well as the diffusion of water out and in the hybrid layer.

Regarding the appearance of the meso-organisation, low intense diffraction spots start to be detected on the CCD camera 40 s after deposition at RH = 25% (*i.e.* 10 s after the drying line). The diffraction patterns are characteristic of a 2D-hexagonal *p6m* lattice where diffraction spots have an equal interplanar distance of 63.7 Å. From 40 s to 20 min after the deposition, the diffraction spots increase in intensity while their *d*-spacing distances uniformly decrease. After 20 min, the film is exposed to a higher relative humidity of RH = 45%, which induces a significant uniform increase of the diffraction spot

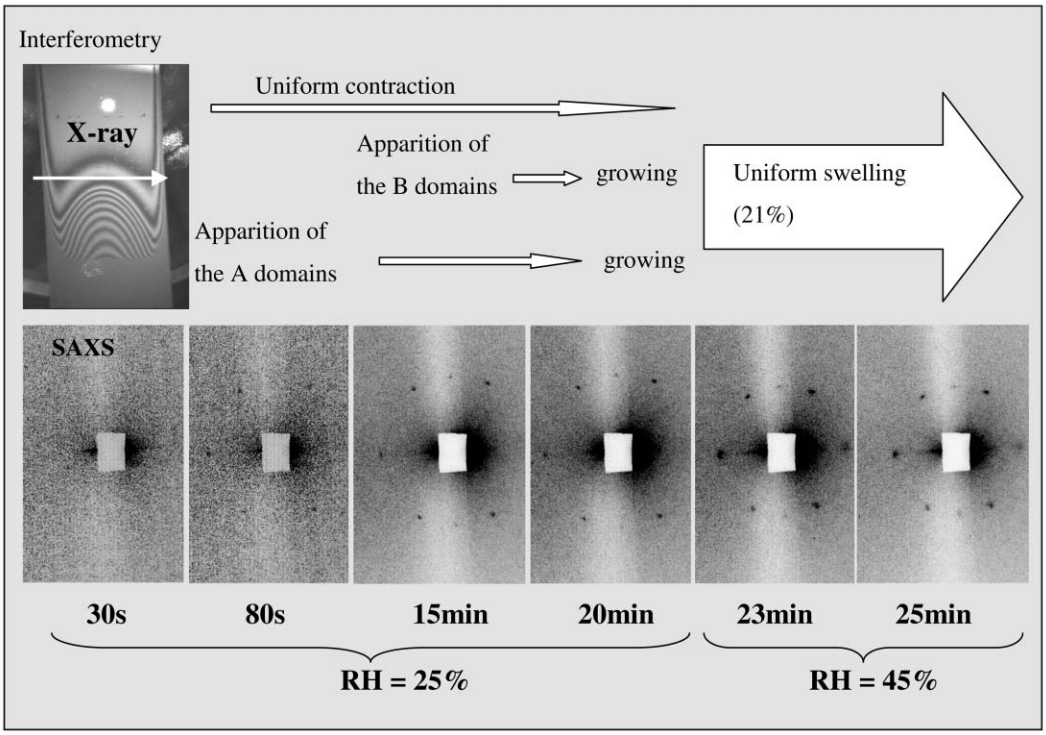

Fig. 3 *In situ* time-resolved SAXS (bottom) and interferometry (upper left) investigations performed on a standard initial solution at RH = 25% humidity during the first 20 min, and RH = 45% humidity after 20 min.

d-spacing. Globally summarised, this results show that the meso-organisation occurs after the drying line, and that drying induces a uniform contraction of the structure while successive exposure to a high humidity atmosphere induces a re-hydration of the film, leading to a uniform swelling of the structure. In order to detail such a formation process, each time-resolved diffraction pattern has been fully analysed as depicted in Fig. 4(a), for the 25 min old film. Diffraction spots, hereafter labelled $A_{[10]}$ and $A_{[01]}$, belong to the same domains for which *a* and *c* axes of the hexagonal array are coplanar to the surface (A domains). In addition, extra diffraction spots labelled B are present and belong to an additional type of domains for which the real structure could not be determined from the single observed diffraction peak (B domains). Fig. 4(b) shows the intensity profile of each diffraction spot contained in the hollow circle represented in Fig. 4(a). In Fig. 4(c) are reported the evolution of the intensity and *d*-spacing of each family of dots, *versus* deposition time, respectively deduced from the intensity circular profile and from the peak to centre distances deduced from each time-resolved diffraction pattern of Fig. 3.

Looking at Fig. 4(a), several observations can be made *via* the interpretation of the peak intensities and position behaviour. One can observe that highly organised (sharp peaks) A domains start to form after 40 s at RH = 25%. Intensities of the $A_{[10]}$ and $A_{[01]}$ peaks similarly increase up to 20 min while the peaks remain highly defined, suggesting that the quantity of matter that organises into a hexagonal mesostructure increases with time to reach its maximum after 20 min. From these observations, it is obvious that the meso-organisation is a progressive process that takes place after the drying line when a relatively low quantity of water and ethanol remains in the layer. In parallel, one observes that B domains start to form 4 min after deposition. The B peak intensity slightly increases up to 20 min as for the $A_{[10]}$ and $A_{[01]}$ ones, but remains quite low, suggesting in a first approximation that fewer B domains are present in the film. The *d*-spacing related to A and B domains have an equal value that is also plotted *versus* deposition time in Fig. 4(c). During the first drying period when RH = 25%, the domains are constantly submitted to a uniform contraction as revealed by the ~15% shrinkage observed after 20 min (from 63.7 to 55.7 Å). When such a film is exposed to a wetter atmosphere (RH = 45%), two phenomena are observed. First, the lattice parameter dramatically increases to 67.5 Å in a uniform fashion, passing *via* the initial value of 63.7 Å. The domains are thus swelling in all the directions when submitted to higher humidity. The second observation concerns the $A_{[01]}$ peak intensity that considerably increases when higher humidity is applied, while the $A_{[10]}$ and B peaks do not change in intensity. In the present geometry only domains that have planes satisfying the Bragg conditions diffract. For example planes that are perfectly aligned with the surface should not diffract as the incident beam is hitting the film with an angle of 4°. However, if a distortion affects the domains, forming wave-like surfaces, the probability of finding parts of domains where planes are in the Bragg conditions is increased. Because of the presence of highly hydrophilic PEO chains, the present films adsorb water when submitted to a higher humidity, which results in a structural

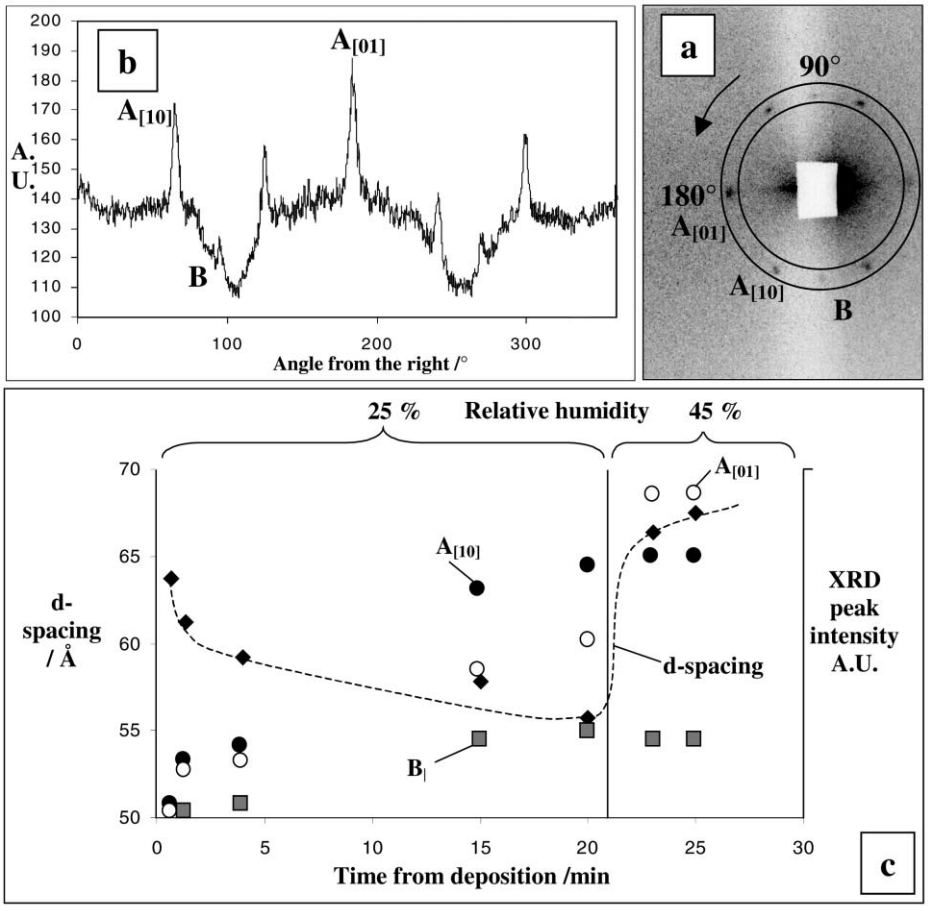

Fig. 4 (a) 2D-XRD pattern corresponding to a typical 2D-hexagonal *p6m* structure from the 25 min old film. (b) Intensity of peaks *versus* angle observed on the SAXS pattern (see hollow circle in (a)). (c) Evolution of diffraction spot *d*-spacing (–♦–) (the variation of *d*-spacing is similar for each spot) and intensities (●: $A_{[10]}$; ○: $A_{[01]}$; ■ B) for both A and B domains, deduced from the time-resolved 2D-XRD patterns shown in Fig. 3 and analysed in details as shown for the 25 min old film pattern in Fig. 4(a) and 4(b).

swelling, also permitted by the uncondensed and flexible aspect of the inorganic framework. This swelling may induce distortions, allowing for some extra planes to align in the Bragg conditions, increasing the corresponding initial peak intensity. As such a phenomenon may also have various plane-distortion intensities, depending on the orientation of planes with respect to the surface, the different observed peaks may not similarly vary in intensity upon such distortions, as it is the case here. Therefore the great variation of the $A_{[01]}$ peak intensity compared to the $A_{[10]}$ and B ones has been attributed to such a water adsorption-induced distortion, that should have more influence on planes coplanar to the interface, with respect to the incident radiation.

4. Discussion

Thin and highly organised optical mesostructured films can be prepared from the solutions described earlier and at a relative humidity below 30%. The preparation route described in this paper gives highly reproducible films from highly stable precursor solutions that can be used several weeks after preparation. Such a stability is explained by the low hydrolysis–condensation degree of inorganic precursors at the initial low pH values (recall the ^{27}Al NMR data). In presence of water and in acidic conditions, hexacoordinated aluminium species are present. Extended hydrolysis of such entities does not occur below a pH of 4–5. Precipitation of aluminium trihydroxide or condensation into aluminium oxyhydroxide can thus not take place in the solution. The solution can be used to prepare mesostructured hybrid films with no influence of the sol ageing time. The fact that these initial inorganic moieties share the solution with the amphiphilic surfactant molecules, should lead to the existence of weak hydrogen and van der Waals interactions between both PEO groups and inorganic intermediates. Upon deposition, an uniform layer of the solution is dragged on the substrate and preferential evaporation of ethanol first takes place, concentrating the system in water, HCl, surfactant, and inorganics. The second evaporation regime drives the departure of water and HCl, and further concentrates the thin film in surfactant and Al derived intermediates. The loss of HCl encourages the further hydrolysis and oligomerisation (partial condensation). However, the evaporation of HCl is far from being total and the film pH remains significantly acidic minutes after deposition, preventing condensation of the inorganic framework. Thereafter, further inorganic condensation occurs when HCl molecules progressively leave the dry film. Moreover a continuous water exchange with the ambient atmosphere helps to modify the pH towards conditions that allow the condensation of the inorganic species. (see swelling behaviour after exposure to higher relative humidity in Fig. 3). This observation was corroborated by RBS measurement that showed only a trace of chloride in a few days old untreated film. The efficient stiffening of the network is mainly achieved along the successive treatments.

Concerning the formation and organisation of micelles into the final mesostructure, the first diffraction peaks appear 10 s after the drying line suggesting that surfactant and inorganic entities self-assemble into the *p6m* structure when the film thickness does not vary significantly any more. The film is mainly composed of inorganic and surfactant molecules, forming a hybrid flexible gel. A rearrangement of the template within the inorganic network must take place at this stage for the well organised structure to be formed. The formation of such films is driven by the condensation/organisation competition. In the present case, the meso-organisation is formed when the system is highly acidic and poorly condensed. The network of the hybrid material is formed of monomers and small oligomers in interaction with PEO groups sub-network by weak hydrogen and van der Waals interactions (see Fig. 5). The PEO groups from co-polymer surfactants have already been shown by Melosh *et al.* to interpenetrate silica walls in SiO_2-based mesostructured materials.[34] In the present case, HCl gradually leaves the layer allowing the pH to slowly increase. However, the inorganic structure is expected to remain flexible (only partly condensed) after a rather longer period of time

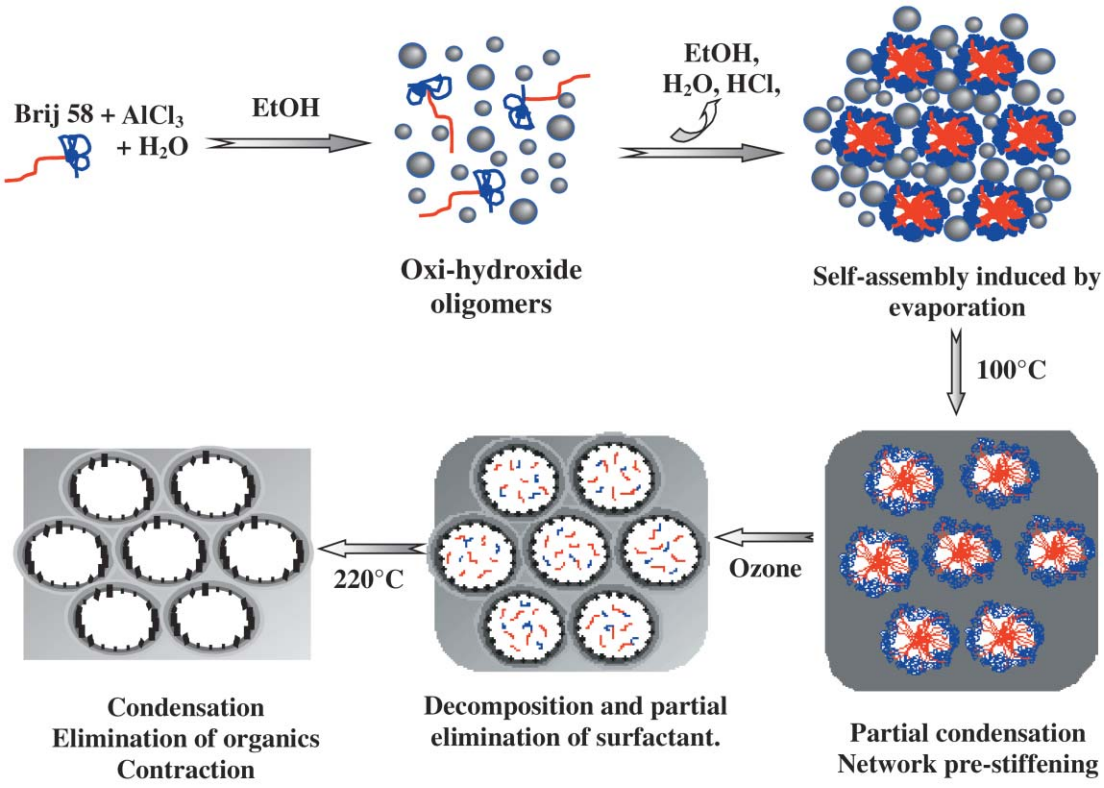

Fig. 5 Schematic representation of the self-assembly process taking place during evaporation.

than with silica materials. It is therefore important to underline here that the meso-organisation is possible only if the condensation is well separated from the self-assembly–organisation. The present system ideally fulfils this requirement as the condensation is slowly permitted by the progressive departure of HCl. As the diffraction peak intensity slowly increases up to 20 min after deposition, the organisation is progressive and may be described as follows. One may expect the surfactant micelles to form first at the air/film interface because the concentration gradient induced by the evaporation is only possible at this interface. Ten seconds after the drying line, cylindrical micelles start to align with the air/film interface forming a first organised layer on the film surface. Then, a 2D-hexagonal phase (A domains), composed of inorganic network surrounding the template phase, starts to grow toward the film centre by self-arrangement of the micelles with the first organised layer and then with the next neighbour organised layer. Such disorder to order transition has also been reported by Yao *et al.* for mesostructured silica films grown from air/solution interfaces.[35]

Four minutes later, the B domains start to form. The B peak intensity remains lower than the A domain diffraction. The structure of this phase could not be determined by 2D-XRD and could not be observed by TEM. However, the B peak *d*-spacing corresponds exactly to the $A_{[01]}$ and $A_{[10]}$ ones, suggesting that the B domains could be *p6m* structured like the A domains, but orientated with an angle of 30° with respect to the A domain orientation, or could be another type of organised domains.

In Fig. 3, one observes that the lattice parameter measured from the XRD patterns dramatically increases up to 21% when a 20 min old film is submitted to a higher relative humidity. A few tens of minutes after swelling, the *p6m* organisation is lost. This suggests that (i) the system is hygroscopic and rapidly takes water from the atmosphere, (ii) the coating is not highly condensed and is flexible enough (low viscosity) to permit a 21% expansion in the three directions of space, (iii) the water is mainly adsorbed in the inorganic/PEO regions[36] as the alkyl centre of the micelles is highly hydrophobic, (iv) the interactions at the hybrid "interface' change through the dilution effect. This interface interaction variation related to the dilution is responsible for the loss of organisation taking place after an induction period of few tens of minutes. Therefore, even if the hybrid structure is flexible once the hexagonal organisation is achieved, no mesomorphic transition may be spontaneously induced by changing the humidity. After swelling, the value of the lattice parameter does not change during the first tens of minutes but the meso-organisation is gradually lost after this. This induction period results from the interpenetration of the PEO chains inside the wall, plugging the micelles to the inorganic phase, preventing easy morphological changes. The *p6m* mesostructure is retained if treatments are applied during this induction period. One may also recall that if no NH_3 is added to the initial solution, the meso-organisation of the as-prepared film is retained only for 1 day at $RH < 30\%$. This period can be increased by adding a small quantity of NH_3 whose role is to favour the early condensation of the aluminium-based intermediate species. It thus is not necessary for obtaining the meso-organisation. Hybrid mesostructure thin films with such a high degree of organisation have been prepared only when the humidity was maintained below 30% during dip-coating. The presence of water, diffusing inside or out of the film depending on HR and the initial solution water content, seems to play a key role in the organisation process as already observed for titania and zirconia films.[14,15,36] At higher relative humidity, worm-like type structures have been obtained suggesting that the higher amount of water present inside the film prevented self-assembly into organised structure either by preventing both phases to ideally interact, or by favouring fast hydrolysis. Water rich systems also tend to evaporate slower than dryer ones. This evaporation rate is likely to play a role in the organisation process. This once more confirms that the formation of a well-defined and well-organised hybrid mesostructure is governed by interactions existing between the inorganic and the organic phases and that the presence of solvent such as water greatly influences the organisation process as well as the evaporation rate.

In order to efficiently remove the surfactant and further condense the inorganic network, a combined thermal and O_3 treatment was applied to the films leading to the final mesoporous 2D-hexagonal organised structure. Care must be taken as the network tends to collapse under fast high temperature treatment. It is thus important to leave the film to slowly condense under mild conditions before applying the treatment. For such a system, we found that the meso-organisation is better retained in the films when they are submitted to 100 °C for 30 min, then allowed to stay 45 min under O_3 atmosphere, and followed by 30 min at 220 °C. The ozone treatment has the aim of removing the organic species (surfactant) and to a certain extent of additionally stiffening the inorganic network.[23,24] XRD investigations of so-treated films showed that the inorganic network remains in an amorphous state.

5. Conclusion

We proposed a simple route to the formation of mesoporous highly organised 2D-hexagonal *p6m* aluminium oxide-based films from $AlCl_3$ precursor and Brij 58 template. The final mesoporous structure is stable up to 220 °C and clearly exhibits 2D-hexagonal organised pores with dimensions ranging from 30 to 40 Å (depending on the direction of contraction). The inorganic framework is likely composed of amorphous aluminium oxyhydroxide. We show that the preparation of such films requires an acidic initial solution and a rapid evaporation process associated with dip-coating. The initial solution remains stable under the low pH conditions used; and can then be liquid-deposited to process films weeks after preparation. The different conditions required along the film formation process for the mesostructure to be formed (*i.e.* stabilisation of initial inorganic entities, evaporation of solvent, self-assembly–organisation followed by inorganic partial condensation) have been suitably governed by adjusting the physicochemical parameters during dip-coating. The obtention of a high degree of organisation requires a low relative humidity during dip-coating and the presence of air/film and film/substrate interfaces. These interfaces tend to drive the structure to self organise with the micelle longer direction coplanar to the interfaces. Once the mesostructure is formed the low relative humidity must be retained in order to prevent alteration of the organisation. If higher humidity is applied, a swelling of the structure induced by water adsorption is first observed, before the structural degradation occurs. Soon after deposition, the interpenetration of the PEO chains within the inorganic walls, may be responsible for the sufficient stability of the hybrid structure, despite the network low degree of condensation and flexibility. Regarding this latter point, treatments have to be applied a maximum of a few tens of minutes after the film preparation. The presented work shows once more that the formation of mesostructured materials is a complex process where ideal conditions have to be adjusted for any system. Through the presented results, the self-assembly phenomena associated with pure Al oxide-based materials have been partially understood, and it would be interesting to investigate if the same mechanisms would apply to other trivalent cations.

Acknowledgement

The authors would like to thank M. Lavergne and Aline Brunet Brunneau for respectively performing the TEM and RBS measurements. The French Institute of Petroleum (IFP) is greatly acknowledged for financial support. G.J.A.A.S.-I. acknowledges financial support from CONICET and Fondación Antorchas (Argentina). E.L.C. acknowledges financial support from the French Ministry of Research and CNPq (Brazil).

References

1 A. Corma, *Chem. Rev.*, 1997, **97**, 2373; A. Corma, *Stud. Surf. Sci. Catal.*, 1998, **117**, 201.
2 C. T. Kresge, M. E. Leonowicz, W. J. Roth, J. C. Vartuli and J. S. Beck, *Nature*, 1992, **359**, 710; J. S. Beck, J. C. Vartuli, W. J. Roth, M. E. Leonowicz, C. T. Kresge, K. D. Schmitt, C. T. W. Chu, D. H. Olson, E. W. Sheppard, S. B. McCullen, J. B. Higgins and J. L. Schlenker, *J. Am. Chem. Soc.*, 1992, **114**, 10834.
3 D. Zhao, Q. Huo, J. Feng, B. F. Chmelka and G. D. Stucky, *J. Am. Chem. Soc.*, 1998, **120**, 6024.
4 N. Melosh, P. Davidson, P. Feng, D. J. Pine and B. F. Chmelka, *J. Am. Chem. Soc.*, 2001, **123**, 1240.
5 S. A. Bagshaw and T. J. Pinnavaia, *Angew. Chem., Int. Ed. Engl.*, 1996, **35**, 1102.
6 S. A. Bagshaw, E. Prouzet and T. J. Pinnavaia, *Science*, 1995, **267**, 865.
7 D. Grosso, A. R. Balkenende, P. A. Albouy, A. Ayral, H. Amenitsch and F. Babonneau, *Chem. Mater.*, 2001, **13**, 1848.
8 C. Sanchez, *Biomimétisme et Matériaux*, Revue de l'observatoire Français des techniques avancés, Série Arago 25, Masson, Paris, 2001.
9 D. Zhao, P. Yang, N. Melosh, J. Feng, B. F. Chmelka and G. D. Stucky, *Adv. Mater.*, 1998, **16**, 1380.
10 M. Klotz, N. Idrissi-Kandri, A. Ayral and C. Guizard, *Mater. Res. Soc. Symp. Proc.*, Materials Research Society, 2000, CC.7.4.
11 Y. Lu, R. Ganguli, C. A. Drewien, M. T. Anderson, C. J. Brinker, W. Gong, Y. Guo, H. Soyez, B. Dunn, M. H. Huang and J. I. Zink, *Nature*, 1997, **389**, 364.
12 D. Grosso, A. R. Balkenende, P. A. Albouy, M. Lavergne and F. Babonneau, *J. Mater. Chem.*, 2000, **10**, 2085.
13 C. J. Brinker, *Curr. Opin. Colloids Interface Sci.*, 1998, **3**, 166.
14 D. Grosso, G. J de A. A. Soler-Illia, F. Babonneau, C. Sanchez, A. Brunet-Bruneau and A. R. Balkenende, *Adv. Mater*, 2001, **13**, 1085.
15 E. L. Crepaldi, G. J de A. A. Soler-Illia, D. Grosso, P. A. Albouy and C. Sanchez, *Chem. Commun.*, 2001, 1582.
16 M. H. Huang, B. S. Dunn and J. I. Zink, *J. Am. Chem. Soc.*, 2000, **122**, 3739.
17 D. Grosso, F. Babonneau, P. A. Albouy, H. Amenitsch, A. R. Balkenende, A. Brunet-Bruneau and J. Rivory, *Chem. Mater.*, in the press.
18 C. J. Brinker, Y. Lu, A. Sellinger and H. Fan, *Adv. Mater.*, 1999, **11**, 579.
19 H. Yang, N. Coombs, I. Sokolov and G. A. Ozin, *J. Mater. Chem.*, 1997, **7**, 1285.
20 H. Yang, N. Coombs, I. Sokolov and G. A. Ozin, *Nature*, 1996, **381**, 589.
21 S. Cabrera, J. E. Haskouri, J. Alamo, A. Beltran, D. Beltran, S. Mendioroz, M. D. Marcos and P. Amoros, *Adv. Mater.*, 1999, **11**, 379.
22 F. Vaudry, S. Khodabandeh and M. E. Davis, *Chem. Mater.*, 1996, **8**, 1451.
23 T. Clark, J. D. Ruiz, H. Fan, J. Brinker, B. I. Swanson and A. N. Parikh, *Chem. Mater.*, 2000, **12**, 3879.
24 G. Buchel, R. Denoyel, P. L. Llewellyn and J. Rouquerol, *J. Mater. Chem.*, 2001, **11**, 539.
25 D. Kundu, H. S. Zhou and I. Honma, *J. Mater. Sci. Lett.*, 1998, **17**, 2089.
26 M. Klotz, P. A. Albouy, A. Ayral, C. Ménager, D. Grosso, A. Van der Lee, V. Cabuil, F. Babonneau and C. Guizard, *Chem. Mater.*, 2000, **12**, 1721.
27 D. Müller and W. Gessner, *Chem. Phys. Lett.*, 1981, **79**, 59.
28 C. F. Baes Jr. and R. E. Mesmer, *The hydrolysis of Cations*, John Wiley and Sons, New York, 1996, p. 120.
29 K. Nakamoto, *Infrared and Raman Spectra of Inorganic and Coordination Compounds*, 4th edn., John Wiley and Sons, New York, 1986.
30 J. Hernandez, *Thesis*, Pierre et Marie Curie University, Paris, 1997.
31 N. Kimura, J. Umemura and S. Hayashi, *J. Colloid Interface Sci.*, 1996, **182**, 356.
32 M. J. Hudson and J. A. Knowles, *J. Mater. Chem.*, 1996, **6**, 89.
33 *CRC Handbook of Chemistry and Physics*, 64th edn., ed. R. C. Weast, CRC Press, Boca Raton, FL, 1983.
34 N. A. Melosh, P. Lipic, F. S. Bares, F. Wudl, G. D. Stucky, G. H. Fredrickson and B. F. Chmelka, *Macromolecules*, 1999, **32**, 4332.
35 N. Yao, A. Y. Ku, N. Nakagawa, T. Lee, D. A. saville and I. A. Aksay, *Chem. Mater.*, 2000, **12**, 1536.
36 G. J. A. A. Soler-Illia and C. Sanchez, *New J. Chem.*, 2000, **24**, 493.